



**HAL**  
open science

# A high-resolution life cycle impact assessment model for continental freshwater habitat change due to water consumption

Mattia Damiani, Philippe Roux, Eléonore Loiseau, Nicolas Lamouroux, Hervé Pella, Maxime Morel, Ralph K. Rosenbaum

## ► To cite this version:

Mattia Damiani, Philippe Roux, Eléonore Loiseau, Nicolas Lamouroux, Hervé Pella, et al.. A high-resolution life cycle impact assessment model for continental freshwater habitat change due to water consumption. *Science of the Total Environment*, 2021, 782, 10.1016/j.scitotenv.2021.146664. hal-03196321

**HAL Id: hal-03196321**

**<https://hal.inrae.fr/hal-03196321v1>**

Submitted on 24 Apr 2023

**HAL** is a multi-disciplinary open access archive for the deposit and dissemination of scientific research documents, whether they are published or not. The documents may come from teaching and research institutions in France or abroad, or from public or private research centers.

L'archive ouverte pluridisciplinaire **HAL**, est destinée au dépôt et à la diffusion de documents scientifiques de niveau recherche, publiés ou non, émanant des établissements d'enseignement et de recherche français ou étrangers, des laboratoires publics ou privés.



Distributed under a Creative Commons Attribution - NonCommercial - NoDerivatives 4.0 International License

# 1 **A high-resolution life cycle impact assessment model for continental** 2 **freshwater habitat change due to water consumption**

3 *Mattia Damiani<sup>\*ac</sup>, Philippe Roux<sup>a</sup>, Eléonore Loiseau<sup>a</sup>, Nicolas Lamouroux<sup>b</sup>, Hervé Pella<sup>b</sup>,*  
4 *Maxime Morel<sup>b</sup>, Ralph K. Rosenbaum<sup>a</sup>*

5 <sup>a</sup> ITAP, INRAE, Montpellier SupAgro, Univ Montpellier, ELSA Research Group and ELSA-  
6 PACT Industrial Chair, Montpellier, France

7 <sup>b</sup> INRAE Lyon, UR RiverLy, Villeurbanne, France

8 <sup>c</sup> Department of Environmental Sciences, Informatics and Statistics, Ca' Foscari University of  
9 Venice, Mestre-Venezia, Italy

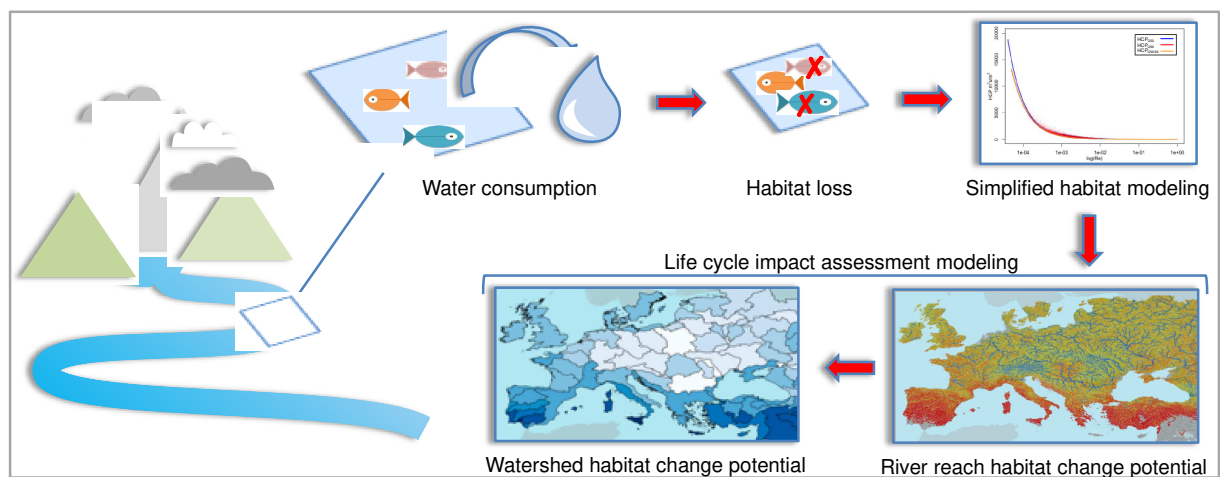
10 <sup>\*</sup>Corresponding author: [damianimtv@gmail.com](mailto:damianimtv@gmail.com)

## 11 **ABSTRACT**

12 Global value chains and climate change have a significant impact on water resources and  
13 increasingly threaten freshwater ecosystems. Recent methodological proposals for life cycle  
14 impact assessment (LCIA), evaluate water use impacts on freshwater habitats based on river  
15 hydraulic parameters alterations. However, they are limited to French rivers due to lack of global  
16 data and models. On this basis, this article proposes an approach to compute regionalized  
17 characterization factors for modeling river habitat change potential (HCP) induced by water  
18 consumption, potentially applicable worldwide. A simplified model is developed for fish guilds  
19 and invertebrates. Based on French datasets, it establishes a relationship between HCP and river  
20 hydraulic parameters. A methodology to derive discharge and hydraulic geometry at the reach  
21 scale is proposed and applied to European and Middle Eastern rivers below 60°N latitude.  
22 Regionalized HCPs are calculated at the river reach scale and aggregated at watershed. Then, the

23 impact of agricultural water use in contrasted European and Middle Eastern countries is  
24 evaluated comparing the outcomes from the HCP and the Available Water Remaining (AWARE)  
25 models at the national scale, considering water supply mix data. The same analysis is carried out  
26 on selected river basins. Finally, result consistency, uncertainty and global applicability of the  
27 overall approach are discussed. The study demonstrates the reproducibility of the impact model  
28 developed for French rivers on any hydrographic network where comparable ecological,  
29 hydrological and hydraulic conditions are met. Furthermore, it highlights the need to characterize  
30 impacts at a higher spatial resolution in areas where HCP is higher. Large scale quantification of  
31 HCP opens the way to the operationalization of mechanistic LCIA models in which the habitat  
32 preferences of freshwater species are taken into account to assess the impacts of water  
33 consumption on biodiversity.

#### 34 **GRAPHICAL ABSTRACT**



35

#### 36 **KEYWORDS**

37 Life cycle impact assessment, water consumption, freshwater habitat, biodiversity

38 **ABBREVIATIONS**

39 LCA, life cycle assessment; LCIA, life cycle impact assessment; CF, characterization factor;  
40 FF, fate factor; EF, effect factor; HCP, habitat change potential; Q, river discharge; CWU,  
41 consumptive water use; HS, habitat suitability; WUA, weighted usable area; Re, Reynolds  
42 number; W, river width ; HB, HydroBASINS; WSmix, water supply mix.

## 43 1. INTRODUCTION

44 Human interaction with water systems in the Anthropocene is being expressed through the  
45 pervasive alteration of the global water cycle. This stimulated the contextualization of watershed  
46 scale management paradigms under a global-scale perspective leading to the production of an  
47 increasing amount of knowledge about worldwide freshwater resource availability and  
48 exploitation (Vörösmarty et al., 2013). Water use for human activities and the exportation of  
49 water-hungry products in globalized supply chains (Dalin et al., 2017; Moran and Kanemoto,  
50 2017), besides the consideration of the geopolitical implications of global water cycle  
51 modification, call for a better understanding of effective and potential consequences on water-  
52 dependent ecosystems.

53 More than 50% of the major river basins on Earth are threatened by pollution and disturbance  
54 of natural flow regimes, with damming, river fragmentation and consumptive water use among  
55 the main causes of biodiversity loss (Vörösmarty et al., 2010). Notwithstanding, estimations of  
56 global river threats and biodiversity status are often partial, since small streams are barely  
57 captured by global statistics, despite being generally more sensitive to anthropic pressures. High  
58 resolution global surface water availability models are nowadays of great importance (Pekel et  
59 al., 2016) and the refinement of methods to assess freshwater requirements of ecosystems and  
60 biodiversity is needed (Janse et al., 2015; Pastor et al., 2014).

61 Life cycle assessment (LCA) is a service and product-oriented approach to global-scale  
62 analysis of supply chains for various impact categories, including water use. Impact indicators  
63 can quantify damage on the environment at the end of a cause-effect chain (i.e. endpoint impact  
64 on resources, human health, and ecosystem quality), or describe environmental mechanisms  
65 occurring prior to the endpoint (i.e. midpoint). Characterization factors are developed to convert

66 inventory data (e.g. m<sup>3</sup> of water consumed per unit of product) to the corresponding impact  
67 indicators. Depending on the type of impact, characterization factors may consider physical  
68 change of local environmental conditions caused by a stressor (fate factor), the exposure of  
69 sensitive targets (exposure factor), and any related adverse effects (effect factor).

70 AWARE, a consensus model for water use impact assessment in LCA, proposed by the  
71 UNEP-SETAC Life Cycle Initiative working group on water use in LCA (WULCA), includes  
72 environmental water requirements (EWR) in the quantification of available water remaining for  
73 life cycle impact assessment (LCIA) midpoint characterization (Boulay et al., 2018). Pfister et al.  
74 (2009) developed endpoint characterization factors for freshwater consumption impacts on net  
75 primary productivity (NPP) of vascular plants as a proxy for species loss. The model proposed  
76 by Verones et al. (2017, 2013a, 2013b) quantifies potential biodiversity impacts for birds,  
77 amphibians, reptiles and mammals in wetlands. Existing LCIA models for riverine species based  
78 on species-discharge relationships (Hanafiah et al., 2011; Tendall et al., 2014) have limitations in  
79 capturing changes in river communities because they do not consider the different responses that  
80 species adapted to different habitats have to river flow reduction or increase (Damiani et al.,  
81 2019, 2018). All these models address furthermore the need for regionalized characterization  
82 factors, further raised, for instance, with recent LCA application at the territorial scale (Loiseau  
83 et al., 2018; Nitschelm et al., 2016), and should ultimately be coupled with spatially explicit  
84 information on water supplies (Leão et al., 2018).

85 Modeling at watershed spatial resolution is consistent with widely employed water  
86 management practices for river ecosystems protection (Palmer et al., 2009). LCIA should  
87 therefore aim at providing global, regionalized models based on mechanistic approaches applied  
88 at watershed and sub-watershed levels. At present, no operational mechanistic model to assess

89 water consumption impacts on stream ecosystems is available at the global scale (Damiani et al.,  
90 2018; Núñez et al., 2016). A high-resolution midpoint impact indicator of habitat change  
91 potential (HCP) based on freshwater physical habitat suitability for fish species, fish guilds and  
92 benthic macroinvertebrates has recently been proposed (Damiani et al., 2019). HCP quantifies  
93 the potential change in available habitat quantity on a river and watershed scale as a result of  
94 water consumption, taking into account the habitat preferences of freshwater fish and  
95 invertebrate species. However, the model is only applicable to the French river network and a  
96 worldwide extension needs to be investigated. The present study builds on this approach  
97 proposing a method for the development of characterization factors for water consumption  
98 impacts on freshwater instream ecosystems, to be implemented worldwide.

99 The availability of global data required to apply the habitat suitability equations adopted in the  
100 local French mechanistic approach is first evaluated. Based on available databases, missing  
101 variables are identified, namely topographical, hydrological and hydraulic. The high-resolution  
102 HCP model is then simplified to reduce complexity of input variables and to adapt to their  
103 availability. Variables are subsequently calculated from existing models to allow implementation  
104 outside France. An application of the new HCP model (referred to as generalized or global HCP  
105 throughout the article) on the European continent and the Middle East is then demonstrated and  
106 discussed. Characterization factors are calculated at the river reach scale and then aggregated at  
107 watershed scale. Results are compared with those of the original local model applied in France  
108 and a case study on European agricultural production is presented to show potential similarities  
109 and dissimilarities between the generalized HCP model and the AWARE model, since it is the  
110 only (proxy-) midpoint method actually including water demand for river ecosystems in the  
111 characterization and providing regionalized characterization factors for watersheds worldwide.

## 112 2. MATERIALS AND METHODS

### 113 2.1 Habitat change potential at river reach scale

114 Characterization factors based on HCP were computed from Equation 1 (taken from Damiani  
115 et al., 2019), where  $CF_i$  is the characterization factor at river reach  $i$ . FF is the fate factor  
116 calculated as the ratio between the difference in river discharge  $dQ$  ( $m^3/s$ ) for each cubic meter of  
117 consumptive water use  $dCWU$  and it is assumed to be equal to 1 (Hanafiah et al., 2011). EF is the  
118 effect factor represented by habitat change potential HCP in  $m^2 s/m^3$  (change in  $m^2$  suitable  
119 habitat quantity induced by river discharge alteration in  $m^3/s$ ), then  $CF = HCP$ . In Damiani et al.  
120 (2019), the authors calculated HCP from seventeen multivariate habitat suitability equations  
121 corresponding to four fish guilds with different habitat preferences, eight fish species where  
122 some of them at different stage of development (i.e. alevin, juvenile, adult; Lamouroux and  
123 Capra, 2002), and a generic equation for benthic macroinvertebrates.

$$CF_i = FF_i \cdot EF_i = \frac{dQ_i}{dCWU_i} \cdot HCP_i \quad (1)$$

124 HCP values were aggregated at reach scale to facilitate their use in LCIA, resulting in two  
125 indicators, one of which gathers guilds and invertebrates HCPs. For a global application of the  
126 model, we adopted the latter since we assume it summarizes a sufficiently large spectrum of  
127 habitat preferences without referring necessarily to particular species for which the distribution  
128 would be uncertain (see Table S1 in Supporting Information – SI – for guilds characteristics).  
129 Nevertheless, in the aggregated characterization factor, fish species favoring shallow and running  
130 waters dominate the overall characterization factor since their habitat is more sensitive to water  
131 quantity alteration.



132 Data availability at the global scale is a major constraint for a worldwide application of the  
 133 HCP model. In Table 1 input variables of the local HCP model are listed.

134 **Table 1.** Variables required to run the HCP model of Damiani et al. (2019)

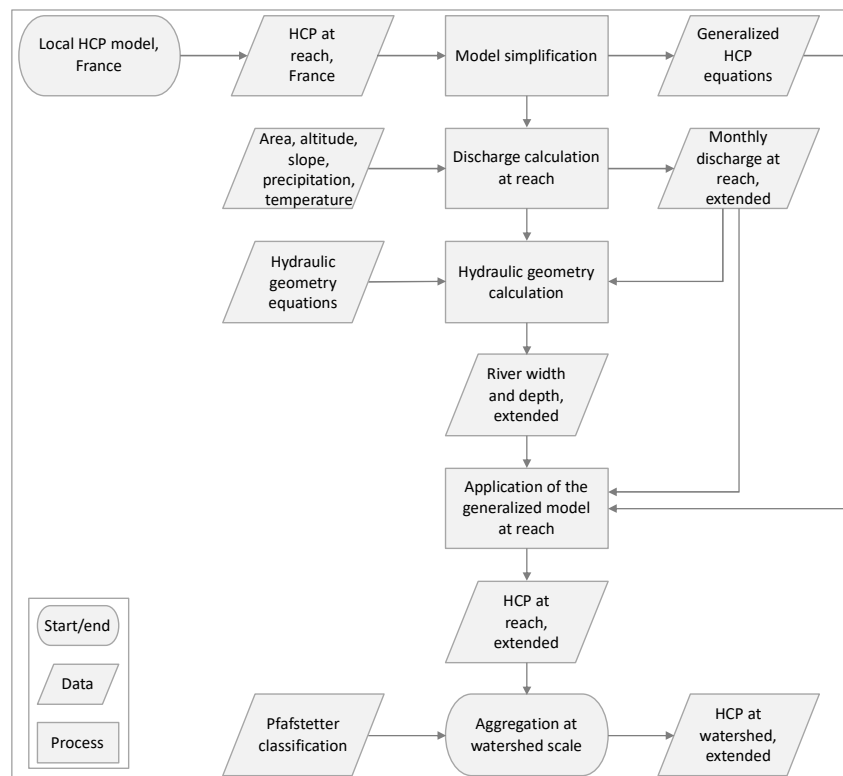
<b>Reach Variable</b>	<b>Unit</b>
Upstream catchment area ( $A$ )	km <sup>2</sup>
Slope ( $S$ )	%
Strahler order ( $O$ )	
Width (calculated from $Q$ , $A$ , $S$ and $O$ )	m
Depth (calculated from $Q$ , $A$ , $S$ and $O$ )	m
Substrate particle diameter	mm
Inter-annual average discharge ( $\bar{Q}$ )	m <sup>3</sup> /s
Inter-annual natural Median daily discharge ( $Q_{50}$ )	m <sup>3</sup> /s
Inter-annual low flow discharge daily percentile ( $Q_{90}$ ), over which daily discharge is 90% of the time	m <sup>3</sup> /s

135

136 The model applied in France in Damiani et al. (2019) is based on the French theoretical  
 137 hydrographical network (RHT, Pella et al., 2012) which has a resolution of the order of meters  
 138 and provides all input variables needed to quantify habitat change potentials. Data in Table 1  
 139 with the same spatial precision are currently not available globally. The products derived from  
 140 the HydroSHEDS database at 15 arc-sec ( $\approx 500$  m at the equator) represent, to our knowledge,  
 141 the best available option in terms of spatial resolution of river segments and global coverage  
 142 (Lehner and Grill, 2013), but hydrological, hydraulic and topographical information are seldom  
 143 associated to such datasets with the same accuracy as in the RHT network.

144 **2.2 Modeling regionalized HCPs worldwide**

145 The difficulty in deriving data at the river reach scale for substrate composition and especially  
 146 for flow magnitudes hinders the global parameterization of HCP (e.g. flow exceedance  
 147 probability for  $Q_{50}$  and  $Q_{90}$  was calculated from daily streamflow data in the RHT network).  
 148 For this reason, a generalization of the local HCP model was developed to reduce the data  
 149 requirements shown in Table 1. Subsequently, input variables of the simplified model were  
 150 calculated for European and Middle Eastern river segments and the results of HCP  
 151 characterization at reach were aggregated at watershed scale (Figure 1).



152

153 **Figure 1.** Logical approach for the characterization of habitat change potential at the global  
 154 scale, demonstrated on European and Middle Eastern rivers

### 155 2.3 Extrapolation of a generalized HCP model

156 Habitat change potential was quantified on French rivers for  $Q_{50}$  and  $Q_{90}$ , representing  
157 median and low flows respectively. The discharge-dependent input variable of the LCIA model,  
158 which is directly altered by water consumption, is the Reynolds number  $Re$ , calculated as the  
159 ratio between river discharge  $Q$  and the product of water viscosity  $\nu$  (considered equal to  $10^{-6}$   
160  $\text{m}^2/\text{s}$ ) and river width  $W$ . To avoid working with high values,  $Re$  is multiplied by  $10^{-7}$  (Damiani  
161 et al., 2019; Lamouroux and Capra, 2002; Lamouroux and Souchon, 2002). Non-linear least  
162 squares analysis was used to fit a power model to HCP results for  $Re$  at  $Q_{50}$  and  $Q_{90}$  (Equations  
163 2 and 3). Model fitting was carried out in R (R Core Team, 2016; RStudio Team, 2016). When  
164 modeling HCP for the world's rivers, defining where and in which period of the year median and  
165 low flow conditions occur is not straightforward. To solve this, an equation was derived by  
166 fitting the model on  $Q_{50}$  and  $Q_{90}$  HCPs together, ranging from -1.8 to 22 396.3  $\text{m}^2 \text{ s}/\text{m}^3$   
167 (Equation 4). The residuals root-mean-squared errors (RMSE) indicate that the average spread of  
168 sample data around the regression line is lower than 0.5% of the HCP range for the three  
169 equations and can thus provide a measure of the goodness of fit of the simplified models.

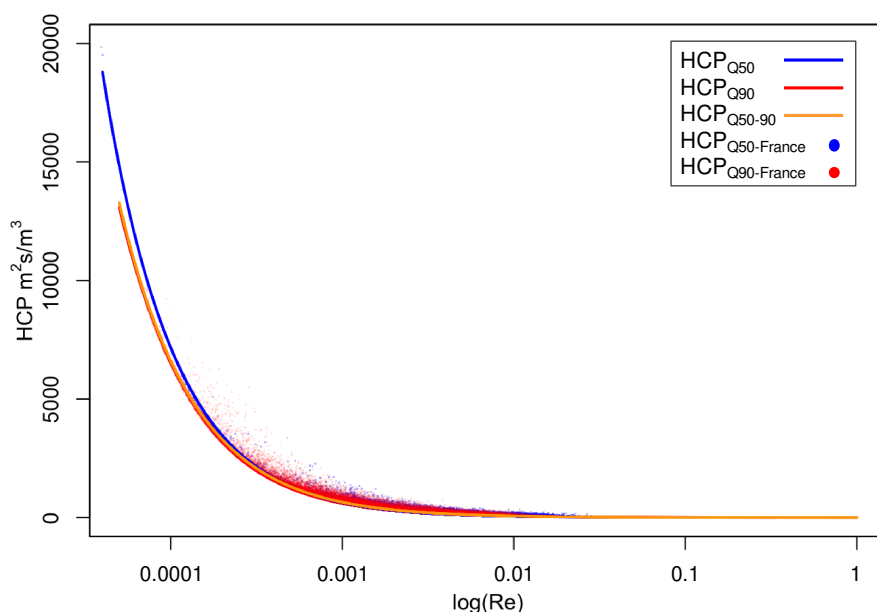
$$HCP_{Q_{50}} = 0.439 \cdot \left( \frac{Q_{50}}{\nu \cdot W_{50}} \right)^{-1.053} \quad \text{RMSE} = 50 \quad (2)$$

$$HCP_{Q_{90}} = 0.669 \cdot \left( \frac{Q_{90}}{\nu \cdot W_{90}} \right)^{-0.998} \quad \text{RMSE} = 108 \quad (3)$$

$$HCP_{Q_{50-90}} = 0.614 \cdot \left( \frac{Q}{\nu \cdot W} \right)^{-1.008} \quad \text{RMSE} = 86 \quad (4)$$

170 In case precise determination of flow exceedance probability is available at the scale of a river  
171 segment, Equation 2 and 3 are preferable, otherwise, and for the present study, the  $HCP_{Q_{50-90}}$   
172 equation was used to calculate characterization factors in Europe and the Middle East.

173 Nonetheless, as shown in Figure 2, results of the three models are not dissimilar, with  $HCP_{Q90}$   
174 and  $HCP_{Q50-90}$  almost overlapping for high HCP values, and the three curves converging as flow  
175 increases.



176  
177 **Figure 2.** Power models describing HCP variation with Reynolds number. Curves fitted on HCP  
178 values at  $Q50$  and  $Q90$  in French rivers

#### 179 2.4 HCP global model's input variables and application at reach scale

180 As demonstrated by the simplified HCP Equations 2, 3, 4, HCP can be calculated globally  
181 from river discharge and width. At present, global flow data estimated at watershed scale are  
182 available (WaterGAP, Alcamo et al., 2003; Döll et al., 2003), a global dataset have been recently  
183 derived from WaterGAP for discharge at river segment scale (Linke et al., 2019), but yet no  $Q50$   
184 and  $Q90$  data are available. A regression model to estimate mean, annual streamflow was  
185 recently proposed based on empirical data from globally distributed gauging stations (Equation  
186 5, adapted from Barbarossa et al., 2017).

$$Q_{it} = 10^{9.066} \cdot A_i^{1.018} \cdot H_i^{-0.509} \cdot S_i^{0.464} \cdot P_{it}^{2.070} \cdot 10^{-0.038 \cdot T_{it}} \quad (5)$$

187 To improve temporal resolution of existing datasets, in this study, this model was used to  
 188 calculate discharge at reach i and month t from the input parameters, listed in Table 2 along with  
 189 the data sources used.

190 **Table 2.** Input data for discharge calculation at river reach (adapted from Barbarossa et al., 2017)

Variable	Unit	Data source	Reference	Resolution	
				Spatial	Temporal
Drainage area (A)	m <sup>2</sup>	A simple global river bankfull width and depth database	Andreadis et al., 2013	15 arc-sec	-
Altitude (H)	m	HydroSHEDS	Lehner and Grill, 2013	15 arc-sec	-
Slope (S)	(°)	HydroSHEDS (calculated)			
Precipitation (P)	m/s	WorldClim	Fick and Hijmans, 2017	30 arc-sec	Month
Temperature (T)	°C	WorldClim			

191

192 Drainage area was taken from the hydraulic geometry dataset of Andreadis et al. (2013) where  
 193 catchment surface values are associated to each river segment present in the HydroSHEDS 15  
 194 arc-sec hydrographic network with river segments in desert areas masked out. Minimum,  
 195 maximum and average altitudes were attributed to each segment based on the HydroSHEDS  
 196 digital elevation model (DEM) at 15 arc-sec. Reach length was also calculated to be able to  
 197 derive average slope in degrees according to Equation 5. A factor of 0.5 which is half of the  
 198 resolution of the DEM, was added to Equation 6 to avoid zero values of slope that would result  
 199 in zero discharge. It was therefore implicitly assumed that with a slope equal to zero, river reach  
 200 discharge is fed by upstream water inertial flow.

$$Slope_i = \arcsin\left(\frac{H_{i\max} - H_{i\min} + 0.5}{Length_i}\right) \cdot \left(\frac{180}{\pi}\right) \quad (6)$$

201 Precipitation and temperature were derived from the WorldClim database at 30 arc-sec  
 202 resolution. Considering that the dataset provides climatic data with a monthly resolution,  
 203 streamflow values ( $Q$ ) were calculated for each month  $t$ , substituting monthly values of  $P$  and  $T$   
 204 in Equation 5. All spatial geoprocessing was carried out using SAGA and QGIS (Conrad et al.,  
 205 2015; Quantum GIS Development Team, 2017).

206 Currently no global databases are available including width ( $W$ ) at the reach scale for monthly  
 207 discharge values. However, hydraulic geometry relationships between discharge, width, depth  
 208 and velocity have been described extensively and, with some approximation depending on the  
 209 chosen method, can be computed by models that remain valid worldwide (Leopold and  
 210 Maddock, 1953; Park, 1977; Rhodes, 1978). In particular, Morel et al. (2020) collected most of  
 211 the hydraulic geometry data available at the scale of stream reaches. They found high  
 212 intercontinental similarity in hydraulic geometry models between France and New Zealand,  
 213 suggesting that their results can be applied globally. Here, to provide global hydraulic geometry  
 214 relationships that represent variations in width  $W$  in space (among reaches) and time (with  
 215 discharge  $Q$ ), we used a combination of the “downstream” (in space) and “at-a-station” (in time)  
 216 formulations of hydraulic geometry of Leopold and Maddock (1953), following the approach of  
 217 Lamouroux and Souchon (2002) and Morel et al. (2020) (Equation 7):

$$W_{it} = \left[ a_d \cdot \bar{Q}_i^{b_d} \right] \cdot \left[ \frac{Q_{it}}{\bar{Q}_i} \right]^b \quad (7)$$

218 where  $a_d$  and  $b_d$  are the “downstream” hydraulic geometry parameters for width, and  $b$  is the  
 219 “at-a-station” exponent that describes variations with discharge. We fitted these three parameters

220 to the data from 1304 reaches of France and New Zealand available in Morel et al. (2020), giving  
221  $a_d = 7.482$ ,  $b_d = 0.477$ , and  $b = 0.148$ .

222 To demonstrate the applicability of the global HCP model at the reach scale, habitat change  
223 potential was quantified on 449 508 river segments covering Europe and the Middle Eastern  
224 regions. Since all variables were calculated on rivers derived from SRTM-based datasets  
225 (NASA's Shuttle Radar Topography Mission), such as HydroSHEDS, the dataset is limited to  
226 rivers below 60°N latitude (taken from Andreadis et al., 2013). The original model developed for  
227 French rivers has limited relevance for high flow periods and, in consequence, the derived global  
228 model as well. Global HCP was calculated using Equation 4 on a monthly basis because for a  
229 large-scale application it is not possible to determine high, median and low flows in regions with  
230 different climate and hydrological conditions. For this reason, it is not possible to exclude some  
231 months a priori from the characterization. This choice is further discussed in section 4.

## 232 **2.5 HCP aggregation at watershed scale**

233 Regionalization of characterization factors is necessary because in LCA it is difficult to obtain  
234 the detail of local water withdrawal and release, especially for background activities and pre-  
235 compiled processes in existing databases, where only average national values are usually  
236 available. With regard to the HCP model, the optimal spatial resolution should be a trade-off  
237 between habitat model uncertainties at the local scale and HCP spatial variability (Damiani et al.,  
238 2019). HCP modeling at watershed level could be the best option in this sense. Reach HCPs were  
239 thus aggregated according to watershed boundaries defined in the HydroBASINS dataset  
240 (Lehner and Grill, 2013) at level 03 and 04 (HB03, HB04), assigning to each river segment the  
241 Pfafstetter codes corresponding to the respective watersheds. The formula used for the

242 aggregated characterization factor at watershed ( $CF_{wt}$ ) was taken from Damiani et al. (2019)  
 243 where the ratio between individual length of river segments and the total length of all catchment  
 244 rivers is the weighting factor for HCPs calculated at reach that are subsequently summed up in an  
 245 aggregated score. However, since high stream order rivers are not included in the European  
 246 database (Strahler order 1 and part of Strahler order 2), we chose to also aggregate based on  
 247 average river water volume  $V$  ( $m^3$ ) per month  $t$  residing in each river segment, as in Equation 8:

$$CF_{wt} = FF_{wt} \cdot EF_{wt} = \frac{dQ_{wt}}{dCWU_{wt}} \cdot \sum_{i=1}^n HCP_{it} \cdot \frac{V_{it}}{\sum_{i=1}^n V_{it}} \quad (8)$$

248 where water volume is the product of width  $W$ , depth  $D$  and length. It was therefore necessary  
 249 to calculate monthly river depth  $D$ , by means of Equation 9, following the same reasoning of  
 250 Equation 7:

$$D_{it} = \left[ c_d \cdot \bar{Q}_i^{f_d} \right] \cdot \left[ \frac{Q_{it}}{\bar{Q}_i} \right]^f \quad (9)$$

251 where  $c_d$  and  $f_d$  are the “downstream” hydraulic geometry parameters for depth, and  $f$  is the  
 252 “at-a-station” exponent ( $c_d = 0.340$ ,  $f_d = 0.259$ ,  $f = 0.292$  from the data in Morel et al., 2020). The  
 253 difference between length and volume weighting is that the first method implies equal weight for  
 254 all reaches in the drainage basin and missing high order streams would likely bias the result of  
 255 the characterization. In the latter the quantity of water that a river provides to the drainage basin  
 256 is the weighting factor. This implies the assumption that the water consumed within a watershed  
 257 has higher probability of being withdrawn from rivers with higher volume of available water.

258 After aggregation, the outputs of the generalized model were compared to those resulting from  
 259 the French model to test results consistency. Four watersheds entirely included into French  
 260 borders were taken into account.  $Q90$  and August characterization factors were compared for the  
 261 local and the generalized model respectively. According to the data used for HCP modeling in



262 this study, August is generally the driest month of the year, with exceptions such as in glacier-fed  
263 streams. It is therefore more likely to have low flows ( $Q_{90}$ ) occurring in this period of the year.

## 264 **2.6 Application to European agricultural water use**

265 The global, regionalized HCP model was applied to a case study to discuss its usability and  
266 interest for LCA. Agriculture alone is responsible for 70% of global water withdrawals  
267 (UNESCO and UN-Water, 2020), 40% in Europe (European Environment Agency, 2018). The  
268 impact of 1 m<sup>3</sup> water consumption for agricultural use according to available agricultural water  
269 supply mixes was assessed (WSmix, Leão et al., 2018). Calculations were made for selected  
270 European countries with agricultural water consumption greater than 1 000 million m<sup>3</sup>/year,  
271 including Turkey and Azerbaijan (SI, Table S4). Since the HCP model applies to surface water  
272 habitats, impact is calculated for the share of surface water in the WSmix. This encompasses  
273 generic surface water consumption data, spring water, inter-basin transferred water and  
274 reservoirs. Although, artificial impoundments per se are not directly covered by the HCP model  
275 which is more sensitive to habitat variation in streams, reservoirs were included because the  
276 differentiation between the two types of water sources was available for a few countries only,  
277 while in most cases the information is hidden in generic surface water use. Moreover, reservoir  
278 water is often used to maintain river flow in dry periods or when water demand is higher, and in  
279 this case can thus be considered as stream water, except that abstraction is delayed in time.  
280 National annual average HCPs were calculated from watershed HCPs of each country and  
281 compared with the AWARE CFs for agriculture at the same spatial and temporal resolution.  
282 AWARE quantifies available water remaining after the demand of humans and aquatic  
283 ecosystems has been met (Boulay et al., 2018). Since Spain had the best detail on watershed and  
284 sub-watershed WSmixes among selected countries in Leão et al. (2018), comparisons between

285 HCP and AWARE were also made at watershed scale for Spanish river basins to discuss spatial  
286 scale choices for HCP characterization (SI, Table S5).

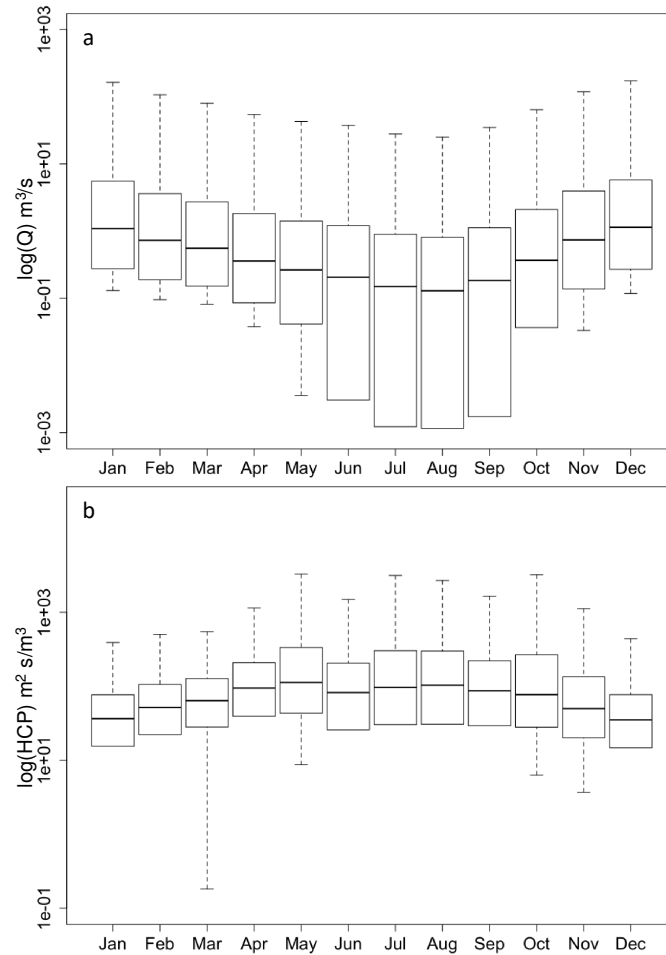
### 287 **3. RESULTS AND DISCUSSION**

#### 288 **3.1 HCP modeling at reach and watershed scale**

289 The mean annual streamflow model applied to European rivers and adjusted with monthly  
290 climatic data, allows estimating the seasonal variability in river discharge along the year,  
291 deriving from rainfall and temperature. Figure 3 represents the detail of monthly  $Q$  and HCP  
292 distribution in the selected rivers excluding extreme values (R robustbase package for skewed  
293 distributions, Hubert and Vandervieren, 2008). Outliers are not represented because of the size of  
294 the data sample and the high variability of European and Middle Eastern climatic conditions and  
295 river regimes. The latter would result in extremely low discharge values for small rivers in dry  
296 periods (e.g. small streams in the Mediterranean region and the Middle East) and six orders of  
297 magnitude greater flows in big rivers during wet months (e.g. in major rivers of continental  
298 Europe). For each month, streamflow distribution is right skewed with maximum median and  
299 average values of 1.03 m<sup>3</sup>/s and 61.58 m<sup>3</sup>/s respectively (both in December), reflecting the  
300 predominance of small streams in the modeling dataset.

301 A reduction in river discharge in dry months is associated to a lower average Reynolds number  
302 in river reaches and therefore to higher habitat change potential for those habitats more likely to  
303 be damaged by water deprivation (shallow and well oxygenated running waters). Figure 3  
304 confirms the lower availability of water in summer months and the associated higher habitat  
305 sensitivity to water consumption. In wet season, indicatively from November to April, 95% of  
306 European rivers included in the study fall between discharge values of 0 and 299.6 m<sup>3</sup>/s. From

307 May to October  $Q$  is between 0 and 37.4  $\text{m}^3/\text{s}$ . The derived HCP is comprised between 0 and  
308 4 070.9  $\text{m}^2 \text{ s}/\text{m}^3$  in wet months and between 0 and 13 352.9  $\text{m}^2 \text{ s}/\text{m}^3$  in dry season (see SI, Tables  
309 S2 and S3).



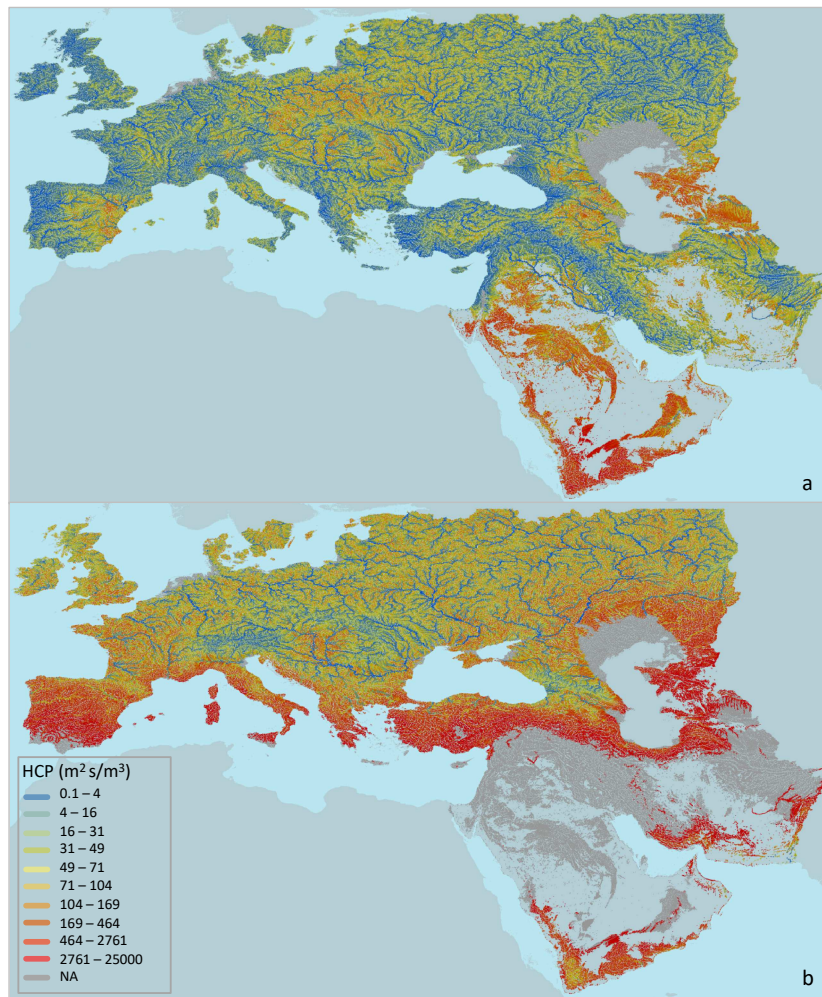
310  
311 **Figure 3.** Monthly discharge  $Q$  in European rivers (a) and HCP characterization factors  
312 distribution (b)

313 Figure 4 illustrates HCP in European and Middle Eastern reaches in January and July.  
314 Characterization factors of the other months are shown in SI, Figure S1. The results highlight an  
315 increase of habitat change potential in dry season, especially in the Mediterranean region and  
316 diffusely in arid areas of the Middle East and the Caspian Sea (Kazakhstan, Turkmenistan, Iran).

317 Dark grey-shaded river segments are those where the HCP model cannot be applied for different  
318 reasons. Overall, HCP greater than 25 000 m<sup>2</sup> s/m<sup>3</sup> were considered outside the validity range of  
319 the habitat model, according to the scores obtained in the local HCP model (Damiani et al.,  
320 2019) from which the generalized model was derived. The maximum amount of such values was  
321 observed in August for 44 860 river segments corresponding to 10% of the total. These streams  
322 are located essentially in the Middle East and in desert regions, corroborating the non-  
323 applicability of the model since it has been developed from river ecosystems pertaining to  
324 different climatic regions and hydrological conditions.

325 A characterization factor is also not quantifiable in rivers where discharge is equal to 0.  
326 According to the formula used to quantify  $Q$ , described in section 2, this may happen for two  
327 reasons. The first one is for reaches that are not sustained by runoff fed from rainfall and that  
328 cease to flow periodically (Figure 4b). In the modeled dataset this applies to 12.8% of river  
329 segments maximum in September, mostly in arid and desert areas. In this case, the global HCP  
330 model is not applicable since rivers dry out and no habitat is present. Moreover, it should be  
331 considered that the uncertainty deriving from applying the characterization model on non-  
332 perennial rivers, such as those represented in Figure 4a and masked out in Figure 4b in the  
333 Arabian Peninsula, is high. In Figure 3, the peaks in HCP values in May and October is due to  
334 the fact that precipitation and thus a modest value of discharge can be attributed to these rivers at  
335 the two boundaries between wet and dry season, resulting in high HCP extremes (SI, Table S3  
336 and Figure S1). However, ecosystems of intermittent and ephemeral rivers are still the subject of  
337 extensive research (Leigh et al., 2016) and, although potential physical habitat availability can be  
338 represented by the HCP indicator, these streams are characterized by specific ecological  
339 mechanisms that cannot be exhaustively described by the HCP model.

340 Discharge, and therefore HCP, could not be attributed also in river segments where the altitude  
341 is equal to or lower than 0. These conditions are distinctive in estuarine and brackish areas that  
342 are out of the scope of the HCP model. Even if fish species are not taken into account, impact of  
343 water use on wetland ecosystems is covered by the models proposed by Verones et al. (2013a,  
344 2013b) which can be therefore complementary to our model.

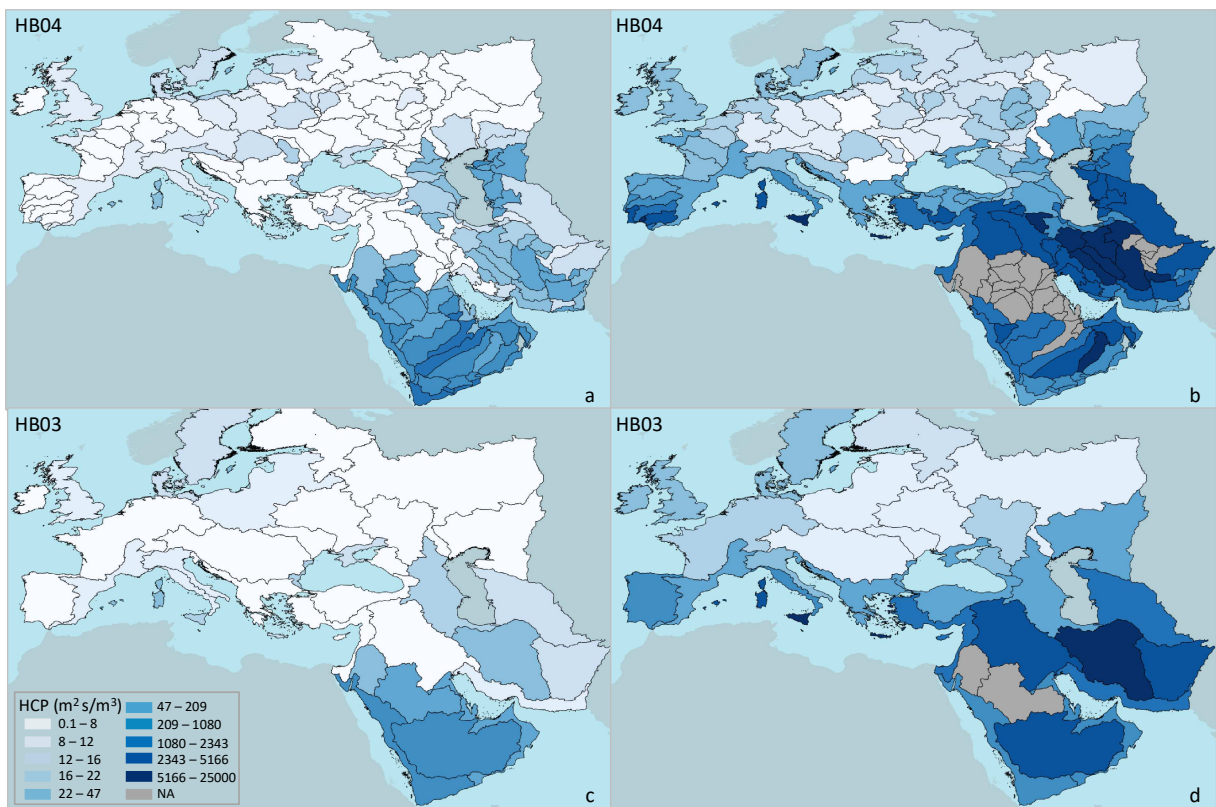


345

346 **Figure 4.** Habitat change potentials in a) January and b) July

347 **3.2 Watershed characterization factors**

348 Aggregated characterization factors at watershed level reflect the outcomes of reach-scale HCP  
349 with higher values during summer months in Mediterranean and arid regions for both  
350 aggregation formulas tested on river lengths and volumes (the latter applied in Figure 4). Higher  
351 level aggregation at HB03 averages the impact of smaller, contiguous sub-watersheds resulting  
352 overall in lower HCP scores. Outcomes of both aggregation methods highlight a decrease of  
353 HCP values when volume weighting is performed, as shown in Table 3.



354  
355 **Figure 5.** Aggregation of reach-scale HCPs based on water volumes in a) January, HB04; b)  
356 July, HB04; c) January, HB03; d) July, HB03

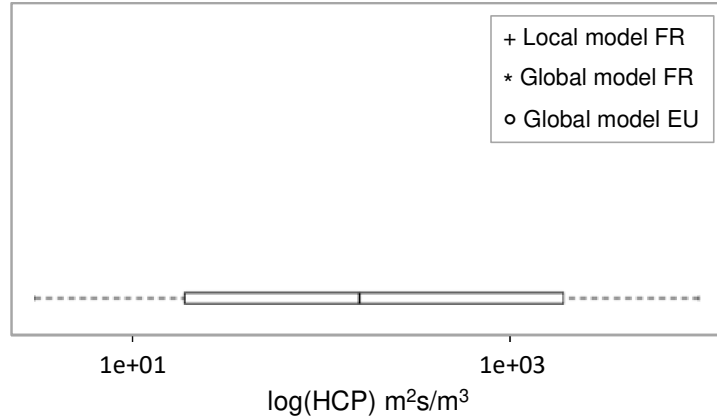
### 357 **3.3 Consistency analysis**

358 In French watersheds at HB04, the comparison between aggregated HCPs on length in the  
359 local model and in the present study showed six times smaller HCP deriving from the  
360 generalized model. This is due to the fact that small, high order streams are missing in the  
361 European database (Strahler orders 1 and 2 with higher HCP) but not in the detailed French RHT  
362 network. Moreover, the relative magnitudes of the characterization value between watersheds are  
363 different in both models. Aggregation on volume is therefore preferable as the relationships  
364 between watersheds remain consistent and the ratio between local and generalized CFs is  
365 decreased to two times when high order streams are taken into account. Recalculating aggregated  
366 CFs from the local French model excluding river segments with Strahler order 1 and 2, resulted  
367 in further reducing the discrepancy with global HCP scores for France, showing very close  
368 characterization factors (Table 3). In absolute terms, these differences are far below the root-  
369 mean-squared error associated to the generalized model in equation 4. Uncertainty resulting from  
370 deriving a generalized model from a spatially limited one, can be attenuated if at-reach  
371 characterization factors are aggregated at watershed scale. Notwithstanding, on a continental  
372 scale the deviation of generalized CFs from local CFs is negligible, as demonstrated in Figure 6  
373 for aggregated HCPs.

374 **Table 3.** Comparison between aggregated HCP scores ( $\text{m}^2 \text{s}/\text{m}^3$ ) for French watersheds from the  
 375 local model (Q90) and the generalized, global characterization model applied to European river  
 376 basins (July)

Pfaf	HCP <sub>l</sub>		HCP <sub>v</sub>				HCP <sub>l</sub>	HCP <sub>v</sub>	HCP <sub>v</sub>	HCP <sub>v</sub>	FR	EU
	FR	EU	FR	FR St>1	FR St>2	EU	FR/EU	FR/EU	FR/EU (FR St>1)	FR/EU (FR St>2)	HCP/ HCP <sub>v</sub>	HCP/ HCP <sub>v</sub>
2321	710.2	144.4	65.8	34.0	25.1	33.8	4.9	1.9	1.0	0.7	10.8	4.3
2322	898.8	126.1	72.6	38.6	28.5	26.9	7.1	2.7	1.4	1.1	12.4	4.7
2323	784.4	153.7	109.5	67.0	47.6	73.9	5.1	1.5	0.9	0.6	7.2	2.1
2324	526.6	99.7	44.4	22.4	17.0	18.8	5.3	2.4	1.2	0.9	11.9	5.3
						$\bar{x}$	5.6	2.1	1.1	0.8	10.5	4.1

377 *Pfaf*: Pfafstetter code from HydroBASINS; *St*: Strahler order; *FR*: local French model; *EU*:  
 378 global model at the European scale; *HCP<sub>l</sub>*: HCP length *l* weighting; *HCP<sub>v</sub>*: HCP volume *v*  
 379 weighting



380  
 381 **Figure 6.** Characterization factors for European watersheds with the detail of French watersheds  
 382 HCP calculated using the generalized (July) and the local model (Q90), including high order  
 383 streams



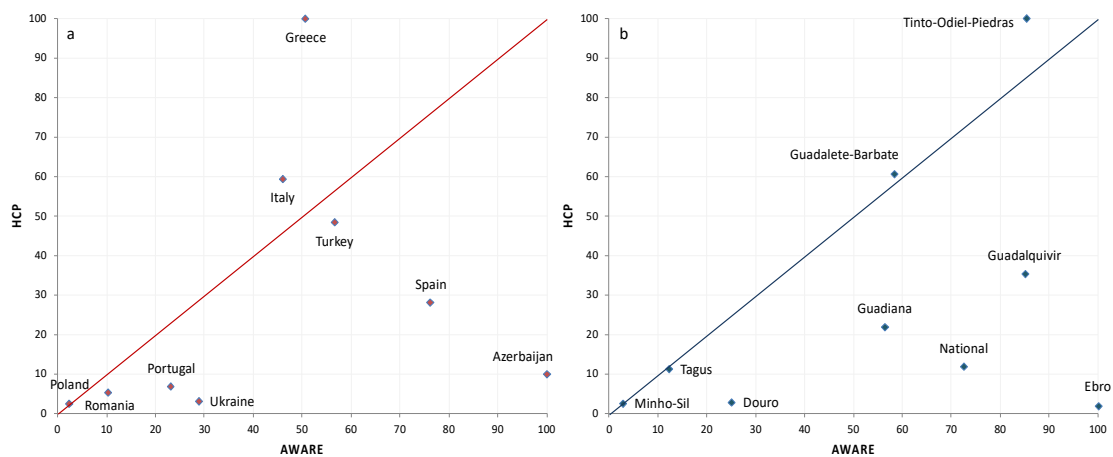
### 384 **3.4 HCP and AWARE for agricultural water use**

385 When comparing AWARE and HCP it should be kept in mind that indicator units are not the  
386 same. While AWARE CFs are dimensionless, the HCP model quantifies the potential alteration  
387 in habitat surface ( $m^2$ ) for marginal discharge change ( $m^3/s$ ). At country scale, the most evident  
388 difference between both characterization approaches depicted in Figure 7a is the country where  
389 consuming  $1 m^3$  of water for agriculture has the greatest impact. AWARE indicates Azerbaijan  
390 as the most impacted country, while the highest HCP is attributed to Greece. This is due to  
391 intrinsic differences of both models. AWARE represents available water remaining net of water  
392 demand by humans and ecosystems (Boulay et al., 2018). As a result, high surface water demand  
393 in Azerbaijan (SI, Table S4) is likely to increase the AWARE score compared to countries where  
394 human water demand is less intense. On the contrary, HCP indicates habitat sensitivity to water  
395 consumption regardless of the use and it is rather dependent on topographical and climatic  
396 conditions. CF for Greece appears therefore higher and heavily influenced by HCP of insular  
397 areas (e.g. Figure 4 and Figure 5). When the water mix is not taken into account and the impact  
398 is allocated on all water sources indifferently, outcomes for Greece are closer in both models (SI,  
399 Figure S2). In Ukraine, a relatively large water demand is the main reason for the difference  
400 between AWARE and the HCP score, according to which stream habitats appear to be less  
401 sensitive to consumptive water use.

402 When corresponding inventory data are available, impact assessment can be brought to  
403 watershed level as illustrated in Figure 7b. The same concept discussed above applies to Spanish  
404 river basins where the Ebro is the most stressed according to AWARE and the Tinto-Odiel-  
405 Piedras catchment shows the highest habitat sensitivity. The HCP value for the Ebro stimulates  
406 reflection on the spatial scales used for HCP aggregation. Values for the Ebro, as well as for

407 other sensitive Spanish river basins such as the Jucar or the Segura included in Figure 4, were  
408 averaged with reach characterization factors of Southern France at HB04 scale (Figure 5). In  
409 critical regions, a narrower spatial resolution could be beneficial to catch the detail of  
410 particularly vulnerable watersheds that would otherwise be lost using large scale characterization  
411 factors.

412



413

414 **Figure 7.** Impact of 1 m<sup>3</sup> consumption of surface water for agriculture according to AWARE and  
415 HCP characterization models at a) country level and b) watershed scale in Spain

#### 416 4. CONCLUSIONS AND RESEARCH OUTLOOK

417 Impact assessment of water consumption through habitat change potential modeling on  
418 individual river segments represents an advancement in terms of environmental relevance and  
419 spatial resolution of water consumption LCIA models. This study demonstrates the  
420 transferability of a high-resolution local HCP model at the continental scale and the validity of  
421 the chosen approach. The new model can be used to develop global characterization factors.  
422 Results at reach scale highlighted the importance of including small streams in the assessment,

423 since they are the most sensitive to water volume change, and the habitats they harbor are  
424 therefore more likely to be affected by consumptive water use.

425 Even if LCA inventories frequently do not support this level of detail, high-resolution  
426 characterization could highlight the uncertainty derived from ignoring spatial variability when  
427 characterizing at lower spatial resolution. On the other hand, if spatially resolved inventory data  
428 are used lower uncertainty could be achieved.

429 In order to facilitate the operationalization of the generalized HCP model, aggregation at  
430 watershed has been carried out. However, in regions where HCP at reach is higher, a more  
431 refined spatial resolution is preferable. On the contrary, for large watersheds in less vulnerable  
432 regions, for instance in Central European river basins, a high level of detail would probably be  
433 excessive and counter-productive in terms of inventory data availability. To allow applicability  
434 of the HCP model in the short-term, country HCPs can be easily calculated and, even if  
435 important details at the watershed scale may be missing, results can be compared with those  
436 deriving from existing models such as AWARE. In addition, some interesting differences were  
437 highlighted between both models demonstrating the interest of HCP characterization as a  
438 complementary indicator focused specifically on assessing impacts on freshwater habitats.

439 The importance of linking inventory data and impact assessment refers as well to the  
440 characterization of water consumption from a temporal point of view. For instance, in the  
441 example discussed above, annual average CFs were associated to annual WSmix. Monthly CFs  
442 are available, but the same detail is not provided by current water consumption data in  
443 inventories. Moreover, reservoir water has been included in generic surface water consumption.  
444 However, reservoirs can be used to ensure sufficient supply of water volumes needed for human  
445 activities and ecosystems in dry season, mitigating water shortage in downstream rivers, which is

446 not taken into account in current models (neither in AWARE nor in the HCP model).  
447 Nonetheless, river regulation and inter-basin transfer may involve non-marginal changes in river  
448 environmental and ecological conditions that would not be covered by the HCP model as it is.

449 Concerning the temporally resolved assessment of HCP, it should also be considered that the  
450 HCP model does not apply to all flow magnitudes. Consequences of a high flow period on  
451 freshwater habitats are different than during low flows. Calculating monthly HCP has been  
452 necessary because it is not possible to define locally when low and high flows occur. However,  
453 monthly discharges used to compute HCP can be still considered averages and therefore high  
454 flow peaks are flattened. An alternative to modeling monthly CF would be to derive median and  
455 minimum discharge for each river segment as a proxy for  $Q_{50}$  and  $Q_{90}$ , and use the resulting  
456 HCP for the wet and the dry season respectively, as done in Damiani et al. (2019). This solution  
457 could also be compared with HCPs from average and minimum discharge modeled in other  
458 existing databases (e.g. Linke et al., 2019). Notwithstanding, the HCP value for high discharge is  
459 extremely low and yet likely to be overestimated because deriving from fitting a model on  
460 median and low flow HCPs. In addition, given the temporal resolution of HCP being monthly,  
461 this is not likely to occur frequently, assuming high flow peaks do not tend to last longer than a  
462 couple of weeks. Furthermore, inventory data are currently not likely to reflect temporal  
463 resolutions beyond trimestral or seasonal resolution and will in most cases be annual averages.  
464 Uncertainty deriving from including potential high flow periods in the characterization is  
465 therefore likely to be negligible in practice.

466 It is also important to mention that water consumption LCA could fully take advantage of  
467 temporal and spatial quantification of water consumption inventory data and impact  
468 characterization, only if inventory and effects are linked by a mechanistic fate factor describing

469 water balance variations in different environmental compartments following withdrawal (e.g.  
470 aquifer, river, soil; Núñez et al., 2018).

471 As a long-term perspective, a mechanistic pathway linking water consumption to a fate factor  
472 and an effect factor based on HCP allows reach-scale, mechanistic, endpoint impact modeling  
473 when combined with information on the biological context at the reach scale. This could include  
474 the presence or absence of species or functional guilds adapted to a certain hydraulic habitat  
475 (considering also their economic, social, and cultural values). A reduction in river discharge in  
476 dry months results in lower average Reynolds number in river reaches and in higher HCP for  
477 those habitats, and therefore those species, more vulnerable to water volume alteration.  
478 Ecohydrological habitat models at the root of the HCP model are derived from empirical, species  
479 abundance data. Relating habitat availability to predicted sensitive species abundance and  
480 density, which is currently subject of extensive research (Lamouroux and Olivier, 2015;  
481 Méricoux et al., 2015), could allow developing LCIA indicators of potential abundance when  
482 hydraulics is the limiting factor. In addition, regarding hydraulic modeling of river habitat, width  
483 and depth equations used in the present study are discharge dependent but can be improved  
484 including geomorphological variables, as for instance catchment slopes, geology or landcover  
485 (Morel et al., 2020).

486 With the purpose of developing global endpoint models based on freshwater habitat change  
487 potential, it is even more crucial to define the range of validity of the model. In the present study,  
488 HCP values greater than  $25\,000\text{ m}^2\text{ s/m}^3$  were excluded. These were mostly associated with  
489 streams in arid and desert regions that are most likely characterized by ecological conditions  
490 different from those on which the HCP model is based. These rivers are predominantly  
491 intermittent and identified calculating discharge at monthly resolution. A better, global

492 characterization of intermittent streams from a hydrologic and ecological perspective would  
493 certainly improve the applicability of the model in the most arid areas. To limit HCP outliers, the  
494 possibility to apply the model on a minimum discharge threshold could also be investigated,  
495 based on hydrology, water users, demographics, or water management policies adopted in certain  
496 regions.

497 It should also be considered that the generalized model has been developed based on local  
498 HCP calculated using habitat preference equations for species that are not ubiquitous. However,  
499 it is assumed that hydrological and hydraulic conditions within validity of the HCP model would  
500 globally determine the establishment of comparable habitats and the presence (or absence) of  
501 species with convergent behavior and habitat preferences (Lamouroux et al., 2002), allowing to  
502 define species archetypes to apply the HCP model at the global level for midpoint and endpoint  
503 LCIA.

#### 504 **ASSOCIATED CONTENT**

505 A Supporting Information document is available including:

- 506 • statistics on modeled streamflow values and HCPs;
- 507 • HCP monthly maps;
- 508 • data used for the AWARE and HCP model comparison.

#### 509 **ACKNOWLEDGEMENTS**

510 The authors are grateful to all members of the ELSA research group for their advice  
511 (Environmental Life Cycle and Sustainability Assessment, <http://www.elsa-lca.org/>). The authors  
512 acknowledge ANR, the Occitanie Region, ONEMA and the industrial partners (BRL, SCP,  
513 SUEZ Groupe, VINADEIS, Compagnie Fruitière) for the financial support of the Industrial

514 Chair for Environmental and Social Sustainability Assessment “ELSA-PACT” (grant no. 13-  
515 CHIN-0005-01).

## 516 REFERENCES

517 Alcamo, J., Döll, P., Henrichs, T., Kaspar, F., Lehner, B., Rösch, T., Siebert, S., 2003.  
518 Development and testing of the WaterGAP 2 global model of water use and availability.  
519 *Hydrol. Sci. J.* 48, 317–337. <https://doi.org/10.1623/hysj.48.3.317.45290>

520 Andreadis, K.M., Schumann, G.J.P., Pavelsky, T., 2013. A simple global river bankfull width  
521 and depth database. *Water Resour. Res.* 49, 7164–7168. <https://doi.org/10.1002/wrcr.20440>

522 Barbarossa, V., Huijbregts, M.A.J., Hendriks, A.J., Beusen, A.H.W., Clavreul, J., King, H.,  
523 Schipper, A.M., 2017. Developing and testing a global-scale regression model to quantify  
524 mean annual streamflow. *J. Hydrol.* 544, 479–487.  
525 <https://doi.org/10.1016/j.jhydrol.2016.11.053>

526 Boulay, A.-M., Bare, J., Benini, L., Berger, M., Lathuilière, M., Manzardo, A., Margni, M.,  
527 Motoshita, M., Núñez, M., Pastor, A. V., Ridoutt, B., Oki, T., Worbe, S., Pfister, S., 2018.  
528 The WULCA consensus characterization model for water scarcity footprints: Assessing  
529 impacts of water consumption based on available water remaining (AWARE). *Int. J. Life*  
530 *Cycle Assess.* 23, 368–378. <https://doi.org/10.1007/s11367-017-1333-8>

531 Conrad, O., Bechtel, B., Bock, M., Dietrich, H., Fischer, E., Gerlitz, L., Wehberg, J., Wichmann,  
532 V., Böhner, J., 2015. System for Automated Geoscientific Analyses (SAGA) v. 2.1.4.  
533 *Geosci. Model Dev.* 8, 1991–2007. <https://doi.org/10.5194/gmd-8-1991-2015>

534 Dalin, C., Wada, Y., Kastner, T., Puma, M.J., 2017. Groundwater depletion embedded in

535 international food trade. *Nature* 543, 700–704. <https://doi.org/10.1038/nature21403>

536 Damiani, M., Lamouroux, N., Pella, H., Roux, P., Loiseau, E., Rosenbaum, R.K., 2019.  
537 Spatialized freshwater ecosystem life cycle impact assessment of water consumption based  
538 on instream habitat change modeling. *Water Res.* 163, 1–12.  
539 <https://doi.org/10.1016/j.watres.2019.114884>

540 Damiani, M., Roux, P., Núñez, M., Loiseau, E., Rosenbaum, R.K., 2018. Addressing water needs  
541 of freshwater ecosystems in life cycle impact assessment of water consumption : state of the  
542 art and applicability of ecohydrological approaches to ecosystem quality characterization.  
543 *Int. J. Life Cycle Assess.* 23, 2071–2088. [https://doi.org/https://doi.org/10.1007/s11367-](https://doi.org/https://doi.org/10.1007/s11367-017-1430-8)  
544 [017-1430-8](https://doi.org/https://doi.org/10.1007/s11367-017-1430-8)

545 Döll, P., Kaspar, F., Lehner, B., 2003. A global hydrological model for deriving water  
546 availability indicators: Model tuning and validation. *J. Hydrol.* 270, 105–134.  
547 [https://doi.org/10.1016/S0022-1694\(02\)00283-4](https://doi.org/10.1016/S0022-1694(02)00283-4)

548 European Environment Agency, 2018. EEA Signals 2018 — Water is life, Eea Signals.  
549 Publications Office of the European Union, Copenhagen. <https://doi.org/10.2800/52469>

550 Fick, S.E., Hijmans, R.J., 2017. WorldClim 2: new 1-km spatial resolution climate surfaces for  
551 global land areas. *Int. J. Climatol.* 37, 4302–4315. <https://doi.org/10.1002/joc.5086>

552 Hanafiah, M.M., Xenopoulos, M. a, Pfister, S., Leuven, R.S.E.W., Huijbregts, M. a J., 2011.  
553 Characterization factors for water consumption and greenhouse gas emission based on  
554 freshwater fish species extinction. *Environ. Sci. Technol.* 45, 5272–5278.

555 Hubert, M., Vandervieren, E., 2008. An adjusted boxplot for skewed distributions. *Comput. Stat.*



556 Data Anal. 52, 5186–5201. <https://doi.org/10.1016/j.csda.2007.11.008>

557 Janse, J.H., Kuiper, J.J., Weijters, M.J., Westerbeek, E.P., Jeuken, M.H.J.L., Bakkenes, M.,  
558 Alkemade, R., Mooij, W.M., Verhoeven, J.T.A., 2015. GLOBIO-Aquatic, a global model of  
559 human impact on the biodiversity of inland aquatic ecosystems. *Environ. Sci. Policy* 48,  
560 99–114. <https://doi.org/10.1016/j.envsci.2014.12.007>

561 Lamouroux, N., Capra, H., 2002. Simple predictions of instream habitat model outputs for target  
562 fish populations. *Freshw. Biol.* 47, 1543–1556. [https://doi.org/10.1046/j.1365-](https://doi.org/10.1046/j.1365-2427.2002.00879.x)  
563 [2427.2002.00879.x](https://doi.org/10.1046/j.1365-2427.2002.00879.x)

564 Lamouroux, N., Olivier, J.M., 2015. Testing predictions of changes in fish abundance and  
565 community structure after flow restoration in four reaches of a large river (French Rhône).  
566 *Freshw. Biol.* 60, 1118–1130. <https://doi.org/10.1111/fwb.12324>

567 Lamouroux, N., Poff, N.L., Angermeier, P.L., 2002. Intercontinental Convergence of Stream  
568 Fish Community Traits Along Geomorphic and Hydraulic Gradients. *Ecology* 83, 1792–  
569 1807. [https://doi.org/10.1890/0012-9658\(2002\)083\[1792:ICOSFC\]2.0.CO;2](https://doi.org/10.1890/0012-9658(2002)083[1792:ICOSFC]2.0.CO;2)

570 Lamouroux, N., Souchon, Y., 2002. Simple predictions of instream habitat model outputs for fish  
571 habitat guilds in large streams. *Freshw. Biol.* 47, 1531–1542. [https://doi.org/10.1046/j.1365-](https://doi.org/10.1046/j.1365-2427.2002.00879.x)  
572 [2427.2002.00879.x](https://doi.org/10.1046/j.1365-2427.2002.00879.x)

573 Leão, S., Roux, P., Núñez, M., Loiseau, E., Junqua, G., Sferratore, A., Penru, Y., Rosenbaum,  
574 R.K., 2018. A worldwide-regionalised water supply mix (WSmix) for life cycle inventory  
575 of water use. *J. Clean. Prod.* 172, 302–313.  
576 <https://doi.org/https://doi.org/10.1016/j.jclepro.2017.10.135>

577 Lehner, B., Grill, G., 2013. Global river hydrography and network routing: baseline data and  
578 new approaches to study the world's large river systems. *Hydrol. Process.* 27, 2171–2186.  
579 <https://doi.org/10.1002/hyp.9740>

580 Leigh, C., Boulton, A.J., Courtwright, J.L., Fritz, K., May, C.L., Walker, R.H., Datry, T., 2016.  
581 Ecological research and management of intermittent rivers: an historical review and future  
582 directions. *Freshw. Biol.* 61, 1181–1199. <https://doi.org/10.1111/fwb.12646>

583 Leopold, L.B., Maddock, T., 1953. *The Hydraulic Geometry of Stream Channels and Some*  
584 *Physiographic Implications*, Geological Survey Professional Paper 252. Washington, DC.

585 Linke, S., Lehner, B., Dallaire, C.O., Ariwi, J., Grill, G., Anand, M., Beames, P., Burchard-  
586 levine, V., Moidu, H., Tan, F., Thieme, M., 2019. HydroATLAS: global hydro-  
587 environmental sub-basin and river reach characteristics at high spatial resolution 0–25.  
588 <https://doi.org/10.1038/s41597-019-0300-6>

589 Loiseau, E., Aissani, L., Le Féon, S., Laurent, F., Cerceau, J., Sala, S., Roux, P., 2018. Territorial  
590 Life Cycle Assessment (LCA): What exactly is it about? A proposal towards using a  
591 common terminology and a research agenda. *J. Clean. Prod.* 176, 474–485.  
592 <https://doi.org/10.1016/j.jclepro.2017.12.169>

593 Méricoux, S., Forcellini, M., Dessaix, J., Fruget, J.F., Lamouroux, N., Statzner, B., 2015. Testing  
594 predictions of changes in benthic invertebrate abundance and community structure after  
595 flow restoration in a large river (French Rhône). *Freshw. Biol.* 60, 1104–1117.  
596 <https://doi.org/10.1111/fwb.12422>

597 Moran, D., Kanemoto, K., 2017. Identifying the Species Threat Hotspots from Global Supply

598 Chains. Nat. Ecol. Evol. 1, 1–5. <https://doi.org/doi:10.1038/s41559-016-0023>

599 Morel, M., Booker, D.J., Gob, F., Lamouroux, N., 2020. Intercontinental predictions of river  
600 hydraulic geometry from catchment physical characteristics. *J. Hydrol.* 582, 124292.  
601 <https://doi.org/10.1016/j.jhydrol.2019.124292>

602 Nitschelm, L., Aubin, J., Corson, M.S., Viaud, V., Walter, C., 2016. Spatial differentiation in  
603 Life Cycle Assessment LCA applied to an agricultural territory: Current practices and  
604 method development. *J. Clean. Prod.* 112, 2472–2484.  
605 <https://doi.org/10.1016/j.jclepro.2015.09.138>

606 Núñez, M., Bouchard, C.R., Bulle, C., Boulay, A.M., Margni, M., 2016. Critical analysis of life  
607 cycle impact assessment methods addressing consequences of freshwater use on ecosystems  
608 and recommendations for future method development. *Int. J. Life Cycle Assess.* 21, 1799–  
609 1815. <https://doi.org/10.1007/s11367-016-1127-4>

610 Núñez, M., Rosenbaum, R.K., Karimpour, S., Boulay, A.-M., Lathuillière, M.J., Margni, M.,  
611 Scherer, L., Verones, F., Pfister, S., 2018. A multimedia hydrological fate modelling  
612 framework to assess water consumption impacts in Life Cycle Assessment. *Environ. Sci.*  
613 *Technol.* 52, 4658–4667. <https://doi.org/10.1021/acs.est.7b05207>

614 Palmer, M.A., Lettenmaier, D.P., Poff, N.L., Postel, S.L., Richter, B., Warner, R., 2009. Climate  
615 change and river ecosystems: Protection and adaptation options. *Environ. Manage.* 44,  
616 1053–1068. <https://doi.org/10.1007/s00267-009-9329-1>

617 Park, C.C., 1977. World-wide variations in hydraulic geometry exponents of stream channels: an  
618 analysis and some observations. *J. Hydrol.* 33, 133–146. [34](https://doi.org/10.1016/0022-</a></p></div><div data-bbox=)

619 1694(77)90103-2

620 Pastor, A. V., Ludwig, F., Biemans, H., Hoff, H., Kabat, P., 2014. Accounting for environmental  
621 flow requirements in global water assessments. *Hydrol. Earth Syst. Sci.* 18, 5041–5059.  
622 <https://doi.org/10.5194/hess-18-5041-2014>

623 Pekel, J., Cottam, A., Gorelick, N., Belward, A.S., 2016. High-resolution mapping of global  
624 surface water and its long-term changes. *Nature* 540, 418–422.  
625 <https://doi.org/10.1038/nature20584>

626 Pella, H., Lejot, J., Lamouroux, N., Snelder, T., 2012. Le réseau hydrographique théorique  
627 (RHT) français et ses attributs environnementaux. *Géomorphologie Reli. Process. Environ.*  
628 18, 317–336. <https://doi.org/10.4000/geomorphologie.9933>

629 Pfister, S., Koehler, A., Hellweg, S., 2009. Assessing the environmental impacts of freshwater  
630 consumption in LCA. *Environ. Sci. Technol.* 43, 4098–4104.  
631 <https://doi.org/10.1021/es802423e>

632 Quantum GIS Development Team, 2017. Quantum GIS Geographic Information System.

633 R Core Team, 2016. R: A language and environment for statistical computing.

634 Rhodes, D.D., 1978. World-wide variations in hydraulic geometry exponents of stream channels:  
635 an analysis and some observations — comments 39, 193–197. <https://doi.org/10.1016/0022->  
636 1694(78)90123-3

637 RStudio Team, 2016. RStudio: integrated development environment for R.

638 Tendall, D.M., Hellweg, S., Pfister, S., Huijbregts, M. a J., Gaillard, G., 2014. Impacts of river

639 water consumption on aquatic biodiversity in life cycle assessment - a proposed method,  
640 and a case study for Europe. *Environ. Sci. Technol.* 48, 3236–44.  
641 <https://doi.org/10.1021/es4048686>

642 UNESCO, UN-Water, 2020. The United Nations World Water Development Report 2020: Water  
643 and Climate Change. Paris.

644 Verones, F., Pfister, S., Hellweg, S., 2013a. Quantifying area changes of internationally  
645 important wetlands due to water consumption in LCA. *Environ. Sci. Technol.* 47, 9799–  
646 9807. <https://doi.org/10.1021/es400266v>

647 Verones, F., Pfister, S., van Zelm, R., Hellweg, S., 2017. Biodiversity impacts from water  
648 consumption on a global scale for use in life cycle assessment. *Int. J. Life Cycle Assess.* 22,  
649 1247–1256. <https://doi.org/10.1007/s11367-016-1236-0>

650 Verones, F., Saner, D., Pfister, S., Baisero, D., Rondinini, C., Hellweg, S., 2013b. Effects of  
651 consumptive water use on biodiversity in wetlands of international importance. *Environ.*  
652 *Sci. Technol.* 47, 12248–12257. <https://doi.org/10.1021/es403635j>

653 Vörösmarty, C.J., McIntyre, P.B., Gessner, M.O., Dudgeon, D., Prusevich, A., Green, P.,  
654 Glidden, S., Bunn, S.E., Sullivan, C.A., Liermann, C.R., Davies, P.M., 2010. Global threats  
655 to human water security and river biodiversity. *Nature* 467, 555–561.  
656 <https://doi.org/doi:10.1038/nature09440>

657 Vörösmarty, C.J., Pahl-Wostl, C., Bunn, S.E., Lawford, R., 2013. Global water, the anthropocene  
658 and the transformation of a science. *Curr. Opin. Environ. Sustain.* 5, 539–550.  
659 <https://doi.org/10.1016/j.cosust.2013.10.005>